Title
X-RAY FLUORESCENCE ANALYSIS OF ACHEX AEROSOLS

Author
Giauque, R.D.

Publication Date
1975-10-01

To be published as a chapter in
Aerosol Characterization Experiments
Hutchinson Memorial, Volume I,
Ann Arbor Press (Expected)

LBL-4414
c.1

X-RAY FLUORESCENCE ANALYSIS OF ACHEX AEROSOLS

R. D. Giauque, L. Y. Goda, and R. B. Garrett

October 21, 1975

Prepared for the U. S. Energy Research and
Development Administration under Contract W-7405-ENG-48

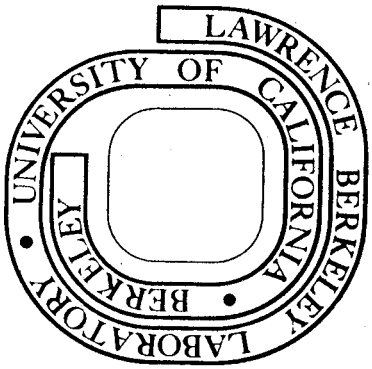

LBL-4414
c.1

DISCLAIMER

LBL-4414

X-RAY FLUORESCENCE ANALYSIS OF ACHEX AEROSOLS

R. D. Giauque, L. Y. Goda, and R. B. Garrett
Lawrence Berkeley Laboratory
Berkeley, California 94720

ABSTRACT

The elemental composition of aerosols collected on filter media and impactor films during the Aerosol Characterization Experiments (ACHEX) were determined by x-ray induced x-ray fluorescence analysis (XRFA). Low power x-ray tubes (<40 watts) and semiconductor detector x-ray spectrometers were utilized for the elemental analyses.

Typically, the concentration of thirteen elements (Al, Si, S, K, Ca, Ti, Mn, Fe, Ni, Zn, Br, Sr, and Pb) were routinely ascertained for aerosols collected for two hour periods. The concentration of twenty-two additional elements determined were usually near or below our detection limits. These programs were sponsored by the California Air Resources Board during the years 1972-1974.

INTRODUCTION

Elemental analysis of aerosols, coupled with meteorological, particle size distribution, gaseous, and other chemical data, provide information which can be used to estimate the contribution of primary and secondary aerosols to the total airborne particulate

matter (1-3). From such data, evaluations of the significance of both natural and anthropogenic sources in the evolution of aerosols may be made. The analytical technique of XRFA lends itself to simultaneous determinations of a broad range of elements in air particulate matter collected on filter media or impactor films. The technique is quantitative, relatively rapid (minutes), and high sensitivities are obtainable (ng/m^3 of air level). Unfortunately, the method does not permit the determination of very low atomic number elements, such as carbon and nitrogen, which are important major constituents of most aerosol specimens. However, the technique is nondestructive and allows subsequent chemical species measurements to be made by alternative analytical procedures.

DISCUSSION OF METHOD

The XRFA method employed for these studies involves the interaction of photons, provided by an x-ray tube either directly or indirectly, with specimen atoms. A fraction of the photons, if of sufficient energy, create inner atomic shell vacancies; subsequent atomic transitions fill the vacancies, and a fraction of these give rise to the emission of characteristic x-rays. These x-rays are detected by a semiconductor detector, sorted by their energies, and the elemental concentrations are determined from the x-ray intensities.

The relative ability to create inner atomic shell vacancies, using various energies of excitation radiations, is determined from the photoelectric cross sections (τ) of the elements. Figure 1 illus-

trates x-ray photoelectric cross section curves for AgLα(3.0 keV), MoKα(17.4 keV), and TbKα(44.2 keV) x-rays (4). As shown, AgLα x-rays are over 2000X more efficient than TbKα x-rays for producing photoelectric interactions with the elements Al → Cl. Likewise, MoKα x-rays are approximately 15X more efficient than TbKα x-rays for producing photoelectric interactions with the elements Al → Sr. TbKα x-rays are efficient for producing photoelectric interactions with the elements Y → La. Consequently, excitation radiations of more than one energy are utilized separately for analysis of a range of elements.

Only a fraction of the vacancies created in a particular energy level are filled by transitions which result in the direct emission of x-rays. Some vacancies are filled by transitions involving the emission of Auger electrons. The fraction of vacancies filled by transitions which directly yield x-rays is known as the fluorescence yield value (ω). Figure 2 shows curves of theoretical values of ω (5,6) for a wide range of elements for the K and L_{III} energy levels. K x-rays are used for the analysis of elements up to atomic number 57 (La) and L x-rays are utilized for the higher atomic number elements. The values of ω are not influenced by the experimental conditions. Low fluorescence yield values and major absorption effect problems either limit sensitivities attainable or prohibit the analysis of very low atomic number elements in aerosol specimens.

Instrumentation and Characteristics

Three different x-ray spectrometers were utilized during these studies to determine the elemental composition of aerosols collected on filter media and impactor films. The characteristics of these spectrometers, as well as a listing of the elements determined by each, are listed in Table I, and the spectrometers are illustrated in Figures 3-6. Both 512 and 1024 channel pulse height analyzers were used to acquire the x-ray spectra. Corrections for system dead times were made using gated clocks that measured the total system live times. More complete descriptions of these spectrometers have been reported (7-9).

Calibration Methods

Aerosols collected on filter media or impactor films can, in general, be considered as thin specimens. For most analyses the concentration of an element, $m_j (\mu g/cm^2)$, is directly proportional to the intensity, I_j, of one of its characteristic K or L x-ray lines and may be expressed as

$$I_j = K_j m_j \qquad (1)$$

where K_j is a sensitivity factor for the element j.

For any given geometry and for constant exciting radiation intensity, the relative ability to excite and detect various x-ray lines from "infinitely" thin specimens may be calculated as previously reported (7). Standardization of a spectrometer for a single element is achieved using a thin-film standard. The standard is prepared thin enough so that absorption effects are negligible ($\sim$100 $\mu g/cm^2$).

Calculated values of K_j for x-ray lines from eight elements have been reported which agree to within several percent of measured values from evaporated thin-film standards (7). In effect, standardization for exciting radiation intensity and total system geometry is made with a single element thin-film standard, and factors converting counts/sec. to $\mu g/cm^2$ for the other elements are calculated.

A thick, pure Si disk is used to standardize spectrometer C for the analyses of the lower Z elements, since a truly thin uniform standard with negligible absorption effects would be difficult to prepare. We define the mass of a thick element disk as

$$m_{thick} = 3.92/(\mu_e \csc\phi_1 + \mu_f \csc\phi_2) \qquad (2)$$

where μ_e and μ_f are the total mass absorption coefficients of the element for the excitation and fluorescence radiations. The angles formed by the excitation and fluorescence radiations with the disk surface are ϕ_1 and ϕ_2, respectively. Since mass m_{thick} represents the mass for which only 25% of the radiation (excitation X fluorescence) is not attenuated, the mass of the disk for calibration purposes equals $m_{thick}/4.0$. We have used thick disks to standardize for Al and S and have obtained agreements to within 5% of the calculated relative excitation-detection efficiency values normalized to Si.

Data Processing

X-ray spectra of the collected aerosol specimens are recorded on magnetic tape and the analytical computations are made by

a Control Data 7600 computer. Although our programs have been established for the analyses of many types of specimens, much less than 50 K of core space would actually be required for the analyses of aerosols only. The analyses programs are performed in three steps. First, the x-ray spectrum background due to the scattered exciting radiation is removed; secondly, the interferences due to overlapping x-ray lines are unfolded, and thirdly, the concentrations of the elements in the original air sampled are calculated from the intensities of the appropriate x-ray lines selected for analysis.

The shape of the scattered exciting radiation background is simply determined by obtaining a spectrum of a blank filter of mass similar to that of the filters used for the aerosol collections. The scattered x-ray background within various energy ranges selected for analysis are ratioed to the intensities of the incoherent scattered exciting radiations. This procedure is possible since the typical aerosol loadings contribute only a couple of percent to the total mass of the filter plus collected aerosol. Also, the loadings are of average effective atomic number similar to that of the collection media.

Fixed sets of channels corresponding to preselected energy ranges are employed for analyses and are verified daily. Minor amplifier adjustments are made, if necessary, to compensate for any slight instrumental deviation such as a base-line or gain shift. To obtain high statistical accuracies, between 70 to 80 percent of the total peak areas are utilized for the analyses. The peak fractions used are established from elemental thin-films. Corrections for overlapping x-ray

lines are also determined from the elemental thin-films by establishing relationship between individual x-ray peak shapes and intensities. In effect, a series of simultaneous equations are established which compensate for overlapping x-ray lines occuring over the preselected energy ranges.

The concentrations of the individual elements present in the aerosol are then calculated from the individual x-ray line intensities using Eq. (3):

$$\frac{\mu g(j)}{m^3} = \frac{C_j}{C_s} \times \frac{m_s}{V} \times \frac{1}{K_j} \times A_j \qquad (3)$$

where

C_j and C_s are the characteristic x-ray count rates from element j and the standard element of known mass

m_s is the standard mass ($\mu g/cm^2$)

V is the volume of air sampled (m^3) per cm^2 of the collection media

K_j is defined by Eq. (1).

A_j is an absorption factor to correct for particle size effects

For most elemental determinations the value of the term A_j is 1.0. Particle size effects must be considered when analyzing for low atomic number elements such as Si and Al. These elements have low energy x-rays, < 4 keV, and are present principally in the large particles, > 2 μ. A fraction of the excitation and fluorescent radiations are attenuated in the individual particles containing these elements. The value of the term A_j is determined experimentally using multiple energies of x-ray excitation which act as variable depth probes. Details of the method are reported elsewhere (9).

RESULTS

Blank Substrata

The different types of collection media utilized during Phase II of the ACHEX program were (1) washed Gelman GA-1 cellulose ester membrane filters for total and after filters of two-hour aerosol specimens, (2) sticky polyethylene films for Lundgren impactor surfaces, (3) Whatman 41 cellulose ester filters for high-volume samples, and (4) glass fiber filters for total and refined aerosol collections for two-hour intervals. Table II lists the concentrations of impurities found in these substrata. Washed GA-1 filters were ascertained to be suitable for most elemental analyses of aerosol specimens due to their relatively low content of impurities. Additionally, they are membrane surface type collection substrata. Zn determinations were not made for aerosols collected on sticky polyethylene due to the high Zn content in the blank. A fraction of the particles collected on Whatman 41 filters are embedded within the substrate. Although Bonner, et al. (10) have estimated absorption corrections for particle penetration, determinations for the elements with K x-rays of energies 3 keV and less were not made. As shown in Table II, the glass fiber filters contained substantial amounts of impurities. Consequently, the concentrations of very few elements (Pb, Br, and in some cases Fe) could be determined for aerosols collected on this media. These filters were used principally to collect aerosols for carbon and extractable organic determinations.

Intercomparisons of Analytical Data

A number of aerosol specimens collected during the ACHEX programs were analyzed for elemental concentrations by both XRFA and instrumental neutron activation analysis (INAA). The INAA were carried out at the Lawrence Livermore Laboratory by R. C. Ragaini and co-workers (11). Although there was some overlap in the elements analyzed by the two techniques (i.e., Al, Ca, Ti, Mn, and Br), the use of both methods permitted the elemental concentrations to be determined for a much broader range of elements. Generally, reasonable agreements were obtained by the two techniques for most analyses, although some discrepancies, which will be discussed, did exist.

Table III shows a comparison of data obtained on high volume aerosol specimens collected during ACHEX II. Two determinations were made by XRFA, one before and one after the INAA. In most cases, the second XRFA yielded lower results which were usually in good agreement with the INAA results. Most likely, the Ca, Ti, and Mn losses can be attributed to physical handling problems during shipment as well as during the INAA. These elements are usually present in the larger particles, > 5 μ. The Br losses might be ascribed to a volatile loss during the INAA.

For aerosol specimens collected for two hour intervals on Gelman GA-1 filters, the discrepencies between the XRFA and INAA results were generally smaller for the large particle elements. This can quite likely be ascribed to the fact that a lower particle size cut point was used during the collection of these specimens.

Elemental Particle Size Distribution Data

Figures 7 and 8 illustrate some of the elemental particle size distribution data obtained during ACHEX II. The Na, Al, and V results were ascertained by INAA. Al, K, Ca, and Fe are predominantly present in the larger particles and are usually thought to originate principally from mechanical processes, such as wind-blown soil dust. S, Ni, Br, and Pb are predominantly present in the submicron size range and originate directly as a result of combustion or indirectly from secondary chemical processes. In California, V in the small particles is generally thought to originate from combustion of fuel oil or from refinery processes. The ratio between V (INAA) and Ni (XRFA) results for eleven after filter specimens collected at the four sites during ACHEX II was $0.77 \pm .04$. Consequently, Ni may well serve as a tracer element equivalent to V in the Los Angeles South Coast Basin.

Tables IV-VII list comparisons of the sums of impactor stages and after filter data versus the total filter data. Typically, during the ACHEX II programs, the sum of the sized aerosol fraction results for elements principally present in small particles (S, Ni, Br, and Pb) agreed to within $\pm$ 15% of the total filter results. However, as much as 50% of the large particles are lost during the collection of the sized aerosol fractions as indicated from the data for the elements which are present mainly in the larger particles (K, Ca, Ti, and Fe). These losses most likely can be attributed to bounce off and wall losses in the Lundgren four stage impactor (12).

Table VIII lists the elements present in California aerosols, which we determined by XRFA during the ACHEX II program. Additionally, the concentrations and the particle size range in which these elements

were typically found are listed. Those elements enclosed in brackets were seldom present at measurable levels. Elemental diurnal patterns were usually established for each episode for the elements S, K, Ca, Ti, Mn, Fe, Ni, Zn, Br, and Pb.

Sensitivities

Tables IX-XI list the sensitivities (3σ values) for the elements determined with each spectrometer. In each case the values listed are for ten minute counting periods. Sensitivities attainable using spectrometer C have subsequently been improved (9). Figures 9-11 are spectra acquired, using each of the spectrometers, of aerosols collected on filter media. The values listed are in ng/cm^2.

SUMMARY

The State of California Air Resources Board sponsored major experiments to study the chemistry and evolution of aerosols in urban and non-urban sites of California. These experiments, which were carried out from 1972-1973, consisted of intensive studies of 24 hour episodes. A number of institutions and laboratories participated in these studies. The programs were carried out under the direction of G. Hidy of the Rockwell International Science Center. The principal objective of the Aerosol Characterization Experiments (ACHEX) were:

1. To characterize the aerosols in terms of their physical and chemical properties.

2. To investigate the evolution of aerosols.

3. To estimate the primary and secondary aerosol contributions to the total airborne particulate concentration.

4. To evaluate the significance of both natural and anthropogenic sources in the evolution of the respirable and visability degrading fractions of aerosols.

Elemental analyses of aerosols collected for two hour intervals during intensive episode studies, together with other chemical, physical, and meteorological data, assisted in studying the evolution of aerosols in California. The elemental data were also used to estimate the contribution of natural, primary, and secondary sources to the total airborne particulate matter. Using X-Ray Fluorescence Analysis (XRFA) techniques 1100 aerosol specimens were analyzed. Diurnal and particle size distribution data were attained for many elements in aerosols collected for two hour intervals. These data assisted in accomplishing the above listed objectives of the ACHEX programs.

ACKNOWLEDGEMENTS

The authors especially want to thank G. Hidy, formerly with the Rockwell International Science Center, for supporting our efforts in the ACHEX programs sponsored by the California Air Resources Board. Appreciation is expressed to F. Goulding, J. Jaklevic and other members of the Nuclear Instrumentation Group for developing and supplying much of the equipment used for these programs. We are indebted to D. Malone for designing the low energy x-ray spectrometer. N. Brown and D. Gok assisted in developing the computer programs employed. We thank J. Hollander for his encouragement in this work. The authors are grateful to J. Wesolowski and B. Appel of the California Department of Public Health for their support and cooperation in this work.

This project was also supported by the U. S. Energy Research and Development Administration.

LITERATURE CITED

1. R. E. Lee, Jr. and D. J. von Lehmden, Trace Metal Pollution in the Environment, J. Air Poll. Cont. Assoc., 23, No. 10, p. 853-857 (1973).

2. G. E. Gordon, W. H. Zoller, E. S. Gladney, and A. G. Jones, Trace Elements in the Urban Atmosphere, Nuclear Methods in Environmental Research, p. 30-37, Proceed. Amer. Nucl. Soc. Topical Meet., August 1971, Univ. of Missouri.

3. S. K. Friedlander, Chemical Element Balances and Identification of Air Pollution Sources, Envir. Sci. and Tech., 7, 235-240 (1973).

4. W. H. McMaster, N. K. Del Grande, J. H. Mellett, and J. H. Hubbell, Compilation of X-Ray Cross Sections, Univ. of California, Lawrence Livermore Laboratory Report UCRL-50174, Section II, Revision I (1969).

5. W. Bambynek, B. Craseman, R. W. Fink, H. U. Freund, H. Mark, C. D. Swift, R. E. Price, and P. Venugopala Rao, X-Ray Fluorescence Yields, Auger, and Coster-Kronig Transistion Probabilities, Rev. of Mod. Phys. 44, No. 4, 716-813 (1972).

6. E. J. McGuire, Atomic L-Shell Coster-Kronig, Auger, and Radiative Rates and Fluorescence Yields for Na-Th, Phys. Rev., A3, 587-594 (1971).

7. R. D. Giauque, F. S. Goulding, J. M. Jaklevic, and R. H. Pehl, Trace Element Determinations With Semiconductor Detector X-Ray Spectrometers, Anal. Chem. 45, 671-681 (1973).

8. F. S. Goulding, J. M. Jaklevic, B. V. Jarrett, D. A. Landis, B. Y. Loo, and J. D. Menge, An Automatic X-Ray Fluorescence Analyzer for Air Particulate Filters, Lawrence Berkeley Laboratory, Berkeley, Calif., Report LBL-1743 (1973).

9. R. D. Giauque, R. B. Garrett, L. Y. Goda, J. M. Jaklevic, and D. F. Malone, Application of a Low Energy X-Ray Spectrometer to Analyses of Suspended Air Particulate Matter, to be published in Proceed. of 24th Annual Denver X-Ray Conf., August 1975, Plenum Press.

10. N. A. Bonner, F. Bazan, and D. C. Camp, Elemental Analysis of Air Filter Samples Using X-Ray Fluorescence, Lawrence Livermore Laboratory, Livermore, Calif., Report UCRL-51388 (1973).

11. R. C. Ragaini, H. R. Ralston, D. Garvis, and R. Kaifer, Trace Elements in California Aerosols, Part 1. Instrumental Neutron Activation Analysis Techniques, Lawrence Livermore Laboratory, Livermore, Calif., Report UCRL-51850 (1975).

12. J. J. Wesolowski, B. R. Appel, and A. Alcocer, The Use of The Lundgren Impactor for Particle Size Measurements, Calif. Dept. of Public Health, Berkeley, Calif., Report AIHL 138 (1973).

Table I.

	Spectrometer A	Spectrometer B	Spectrometer C
Detector	Grounded guard-ring	Guard-ring reject	Top-hat
Electronics	Pulsed-light feedback	Pulsed-light feedback	Pulsed-light feedback
Resolution at 5.9 keV	~ 225 eV	~ 190 eV	~ 175 eV
X-ray tube, power	Mo transmission 20 watts	W, 50 watts	Ag, 50 watts
Excitation method	Direct	Secondary targets	Direct and secondary targets
Total area of specimen analyzed	1-3 cm^2	5 cm^2	1 cm^2
Elements determined	S → Sr, Hg, Pb	Sr → Ba	Mg → Cl

Table II. Blank Filter Impurities ($\mu g/cm^2$) *.

Element	GA-1	Sticky polyethylene	Whatman 41	Glass Fiber
K	N.D.	N.D.	N.D.	42
Ca	0.16	N.D.	0.05	41
Fe	0.031	0.02	0.02	2.6
Cu	0.058	N.D.	0.01	N.D.
Zn	0.004	0.6	0.01	167
Rb	N.D.	N.D.	N.D.	0.41
Sr	N.D.	N.D.	N.D.	0.67
Ba	N.D.	N.D.	N.D.	3.8
Pb	N.D.	N.D.	N.D.	0.12

* Values uncorrected for filter absorption effects.

Table III. Comparison of data determined by XRFA (LBL) and INAA (LLL).

Specimen		Ca	Ti	Mn	Br
TA0151HV	XRF-1	1470 ± 70	210 ± 42	46 ± 4	302 ± 12
	INAA	1329 ± 450	125 ± 50	34 ± 1	259 ± 9
	XRF-2	1120 ± 60	124 ± 36	34 ± 3	252 ± 10
TB0153HV	XRF-1	2060 ± 100	308 ± 85	76 ± 5	749 ± 30
	INAA	2526 ± 660	326 ± 81	58 ± 2	555 ± 16
	XRF-2	1610 ± 80	226 ± 67	59 ± 4	634 ± 25
TC0153HV	XRF-1	2530 ± 130	328 ± 106	83 ± 6	733 ± 29
	INAA	2278 ± 328	301 ± 93	64 ± 2	639 ± 23
	XRF-2	1930 ± 100	240 ± 73	59 ± 5	642 ± 26
TD0154HV	XRF-1	2110 ± 110	270 ± 77	64 ± 6	568 ± 28
	INAA	1843 ± 754	251 ± 92	46 ± 2	521 ± 15
	XRF-2	1700 ± 70	183 ± 52	42 ± 6	534 ± 21
TE0155HV	XRF-1	1340 ± 70	209 ± 28	48 ± 3	221 ± 9
	INAA	1400 ± 484	290 ± 128	34 ± 1	420 ± 15
	XRF-2	984 ± 49	123 ± 32	33 ± 3	407 ± 16
UF0156HV	XRF-1	1890 ± 90	275 ± 61	71 ± 4	473 ± 19
	INAA	2249 ± 247	297 ± 67	59 ± 2	433 ± 16
	XRF-2	1560 ± 80	193 ± 53	58 ± 4	432 ± 17
VH0158HV	XRF-1	3780 ± 190	289 ± 43	92 ± 4	289 ± 12
	INAA	4764 ± 369	219 ± 63	80 ± 3	217 ± 6
	XRF-2	3240 ± 160	192 ± 44	80 ± 4	257 ± 10
V10159HV	XRF-1	3730 ± 190	300 ± 42	89 ± 4	312 ± 12
	INAA	4705 ± 376	355 ± 65	74 ± 2	260 ± 9
	XRF-2	2980 ± 150	194 ± 50	72 ± 4	269 ± 11
VJ0160HV	XRF-1	3150 ± 160	384 ± 46	86 ± 5	162 ± 6
	INAA	2706 ± 321	265 ± 64		131 ± 4
	XRF-2	1810 ± 90	185 ± 28	42 ± 4	130 ± 5
WK0161HV	XRF-1	1280 ± 60	152 ± 85	42 ± 3	251 ± 10
	INAA	1308 ± 70	181 ± 56	40 ± 1	203 ± 6
	XRF-2	1120 ± 60	114 ± 81	37 ± 3	223 ± 9
WL0163HV	XRF-1	1450 ± 70	199 ± 44	54 ± 4	1190 ± 50
	INAA	1936 ± 60	< 148	44 ± 2	1212 ± 34
	XRF-2	1100 ± 60	125 ± 51	40 ± 3	1140 ± 50

Table IV. Elemental aerosol size fraction data (ng/m^3).

West Covina - episode TB 7-24-73 1200-1400

Stage	μ	S	K	Ca	Ti	Mn	Fe	Ni	Br	Pb
1	12.4	<400	329±38	395±60	79±7	5±2	916±31	<3	27±2	52±3
2	5.6	<400	107±27	204±57	17±6	3±2	344±13	<3	21±1	42±3
3	2.5	460±160	171±27	325±59	29±6	4±2	388±16	<4	53±2	184±7
4	0.9	3200±300	<78	<60	<15	<7	104±4	5±1	107±4	396±16
AF	0.2	10500±1500	303±59	166±30	<40	9±5	306±12	41±3	488±20	2930±120
Σ(1→AF)		14200	910	1090	125	21	2060	46	696	3600
TF		15200±1500	1690±80	2090±80	392±98	93±7	3580±140	53±4	735±29	3890±150
Σ(1→AF)/TF		.93	.54	.52	.32	.23	.57	.87	.95	.93

Table V. Elemental aerosol size fraction data (ng/m^3)

Pomona - episode UF 8-17-73 1200-1400

Stage	μ	S	K	Ca	Ti	Mn	Fe	Ni	Br	Pb
1	12.4	<400	512±51	682±34	177±25	23±4	1360±50	5±2	24±3	87±4
2	5.6	<400	100±28	172±17	26±5	7±3	242±10	3±1	20±2	53±2
3	2.5	820±160	153±28	214±17	40±17	10±3	374±15	4±1	51±2	187±8
4	0.9	5500±600	113±28	58±15	<18	5±3	136±5	8±1	140±6	593±24
AF	0.2	7500±800	<156	35±29	<35	20±5	167±7	47±3	272±11	2020±80
Σ(1→AF)		13800	878	1160	243	65	2280	67	507	2940
TF		12300±1200	1150±120	2110±80	395±94	84±7	3420±140	67±4	507±20	3020±120
Σ(1→AF)/TF		1.12	.76	.55	.62	.77	.67	1.00	1.00	.97

Table VI. Elemental aerosol size fraction data (ng/m^3)

Rubidoux - episode VH 10-6-73 1200-1400

Stage	μ	S	K	Ca	Ti	Mn	Fe	Ni	Br	Pb
1	12.4	<400	494±43	825±34	103±13	19±4	951±30	2±1	12±2	32±3
2	5.6	<400	207±28	400±20	44±17	7±2	386±16	<3	12±2	36±2
3	2.5	<400	179±29	453±23	44±6	8±3	349±14	2±1	24±2	93±4
4	0.9	1300±200	98±27	63±15	<15	<7	56±3	4±1	59±2	244±10
AF	0.2	2600±400	<156	107±29	<24	<12	94±5	6±2	145±6	867±35
Σ(1→AF)		3900	978	1850	191	34	1840	14	252	1270
TF		5300±500	1370±140	3280±130	340±39	69±6	3150±130	10±3	294±12	1500±60
Σ(1→AF)/TF		.74	.71	.56	.56	.49	.58	1.4	.86	.85

Table VII. Elemental aerosol size fraction data (ng/m^3)

Dominguez Hills - episode WL 10-11-73 1200-1400

Stage	μ	S	K	Ca	Ti	Mn	Fe	Ni	Br	Pb
1	12.4	<400	87±38	137±21	29±12	3±2	192±6	3±1	17±2	34±3
2	5.6	<400	76±27	101±16	14±10	<7	93±4	2±1	12±2	28±2
3	2.5	<400	112±28	114±16	21±5	<7	91±4	4±1	30±2	57±3
4	0.9	350±150	<83	41±15	<15	4±2	58±3	4±1	39±2	102±4
AF	0.2	2900±400	<178	84±29	<31	13±5	81±5	51±3	160±6	782±31
Σ(1→AF)		3300	275	477	64	20	515	64	258	1000
TF		4400±400	220±68	424±37	<89	26±6	561±22	80±4	220±9	1130±50
Σ(1→AF)/TF		.75	1.25	1.13	-	.77	.92	.80	1.17	.89

Table VIII. California Urban Aerosols

Particle diameter	> 1μ	< 1μ
Conc. range ($\mu g/m^3$)		
> 1	Al, Si, Ca, Fe	S, Pb
0.1 - 1	K, Ti, Zn, (S)	Ca, Fe, Br, (K)
0.01 - 0.1	Cr, Mn, Br, Sr, Pb, (Ba)	Ti, Ni, Cu, Zn, (V), (As), (Sn), (Sb), (I)
0.001- 0.01	Ni, Cu, (Ga), (Rb)	Mn, (Se), (Cd)

Table IX. Theoretical Limits of Detection, Spectrometer A

Media	Gelman GA-1	Sticky polyethylene
Mass (mg/cm^2)	5.0	5.0
Air volume sampled (m^3/cm^2)	0.75	2.40
Area analyzed (cm^2)	3	1
Element and spectral line		
SKα	900 ng/m^3	480 ng/m^3
ClKα	420	220
KKα	140	100
CaKα	65	55
TiKα	26	19
VKα	21	15
CrKα	17	10
MnKα	12	8
FeKα	13	10
NiKα	5	5
CuKα	8	5
ZnKα	5	12
GaKα	4	5
AsKα	5	4
SeKα	5	4
BrKα	7	5
RbKα	10	8

continued

Table IX continued

Media	Gelman GA-1	Sticky polyethylene
SrKα	12	9
HgLα	9	7
PbLα	9	7
PbLβ	23	19

Table X. Theoretical Limits of Detection, Spectrometer B
Tb Secondary Target

Media	Whatman-41
Mass (mg/cm^2)	9.0
Air volume sampled (m^3/cm^2)	3.0
Area Analyzed (cm^2)	4
Element and spectral line	
SrKα	17 ng/m^3
YKα	16
ZrKα	14
NbKα	12
MoKα	11
PdKα	10
AgKα	9
CdKα	10
InKα	12
SnKα	13
SbKα	13
TeKα	14
IKα	17
CsKα	28
BaKα	38
LaKα	56

Table XI. Theoretical Limits of Detection, Spectrometer C

Media	Gelman GA-1			
Mass (mg/cm^2)	5.0			
Air volume sampled (m^3/cm^2)	0.75			
Area analyzed (cm^2)	1			
Mode	Zr secondary target	Ag secondary target	Ni secondary target	Direct, Ag filter
Element and spectral line				
MgKα	-	-	-	320 ng/m^3
AlKα	900	1400	7200	130
SiKα	560	700	3500	70
SKα	-	400	1400	40
ClKα	-	370	900	40
CaKα	-	-	200	-
TiKα	-	-	130	-
FeKα	-	-	120	-

FIGURE CAPTIONS

Fig. 1. Photoelectric cross section curves for 3.0, 17.4, and 44.2 keV photons.

Fig. 2. Theoretical fluorescence yield curves for the K and L_{III} energy levels.

Fig. 3. Spectrometer A. X-ray fluorescence analysis technique employing direct excitation using a Mo transmission x-ray tube.

Fig. 4. Spectrometer B. X-ray fluorescence analysis technique using a W anode x-ray tube and secondary targets to provide the exciting radiation.
(Goulding-Jaklevic, E.P.A. type x-ray spectrometer).

Fig. 5. Spectrometer C. X-ray fluorescence analysis technique by direct excitation using a Ag anode x-ray tube.

Fig. 6. Spectrometer C. X-ray fluorescence analysis technique with a Ag anode x-ray tube and secondary targets to provide the exciting radiation.

Fig. 7. Elemental particle size distribution data for aerosol collected at Rubidoux on 9/19/73 between 1200-1400.

Fig. 8. Elemental particle size distribution data for aerosol collected at Dominguez Hills on 10/5/73 between 1000-1200.

Fig. 9. Spectrum of a total filter aerosol specimen collected for a two hour interval. Spectrum obtained using spectrometer A.

Fig. 10. Spectrum of a Hi-Vol aerosol specimen collected for a 24 hour period. Spectrum obtained using spectrometer B.

Fig. 11. Spectrum of a total filter aerosol specimen collected for a two hour interval. Spectrum obtained using spectrometer C in the direct excitation mode.

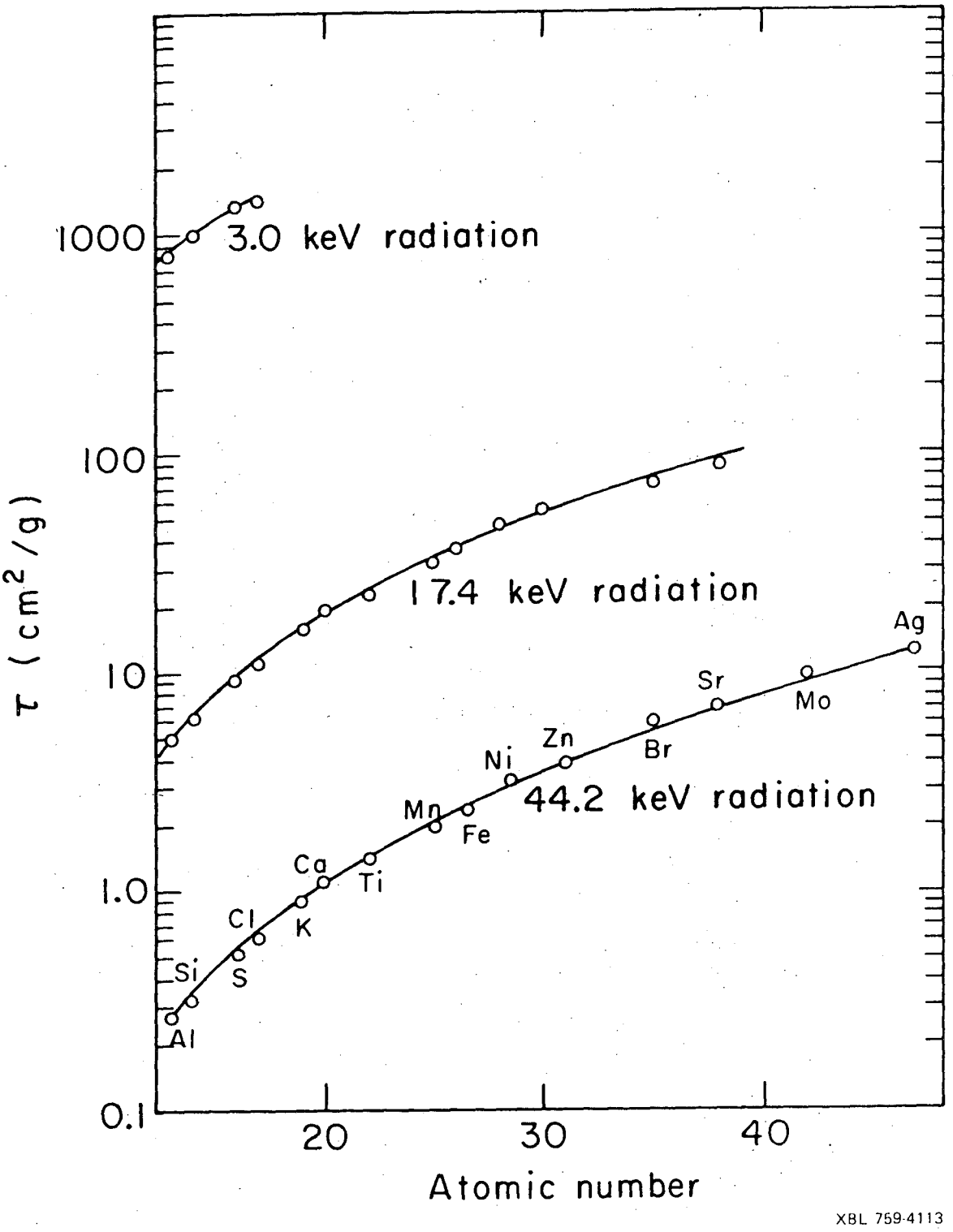
1000
100
10
1.0
0.1
τ (cm²/g)
3.0 keV radiation
17.4 keV radiation
44.2 keV radiation
Al
Si
S
Cl
K
Ca
Ti
Mn
Fe
Ni
Zn
Br
Sr
Mo
Ag
20
30
40
Atomic number
XBL 759-4113

Fig. 1

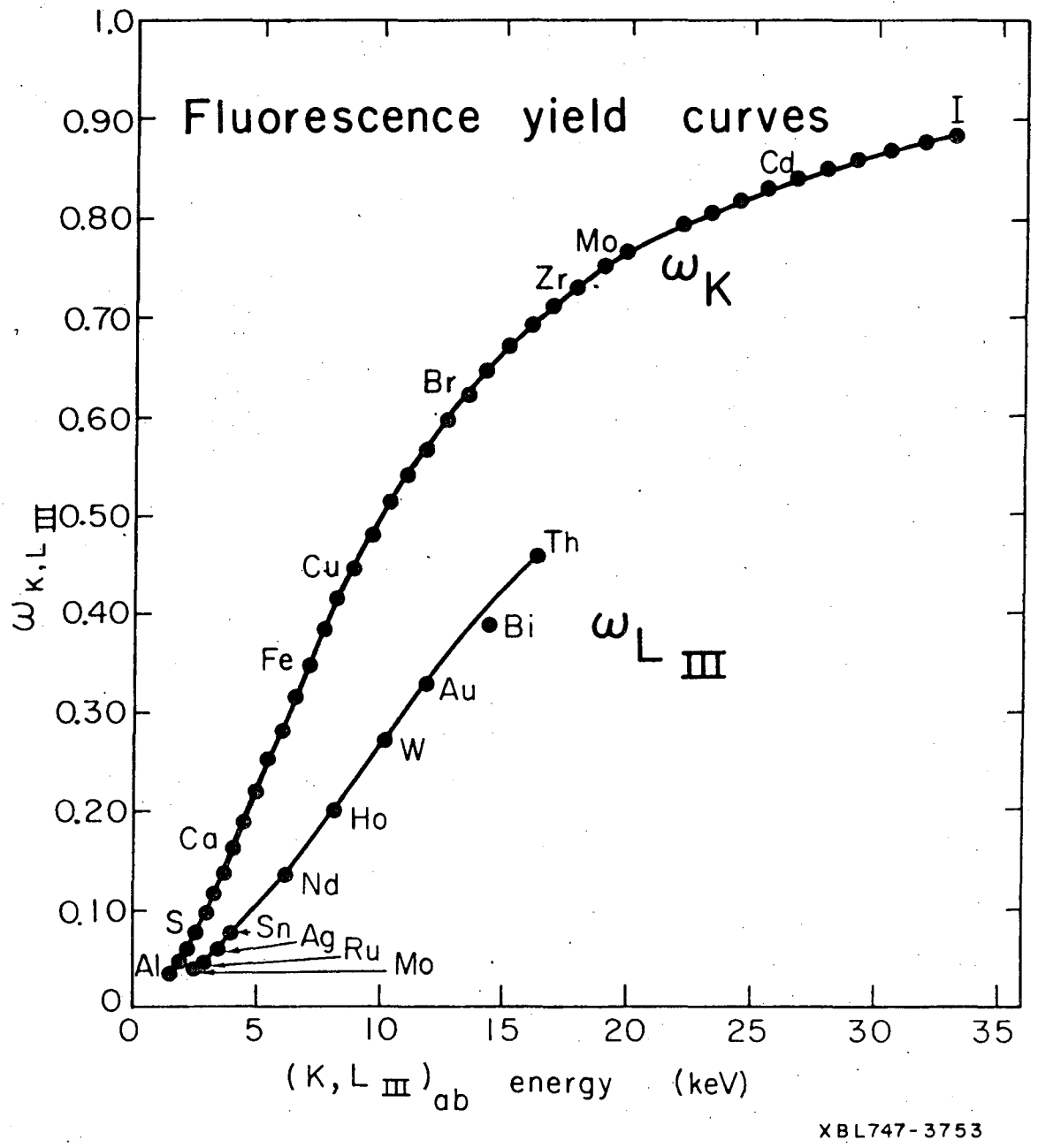
Fluorescence yield curves
ω_K
$\omega_{L\,III}$
$\omega_{K,L\,III}$
$(K, L_{III})_{ab}$ energy (keV)
I
Cd
Mo
Zr
Br
Cu
Fe
Ca
S
Al
Sn
Ag
Ru
Mo
Th
Bi
Au
W
Ho
Nd
1.0
0.90
0.80
0.70
0.60
0.50
0.40
0.30
0.20
0.10
0
0
5
10
15
20
25
30
35
XBL747-3753

Fig. 2

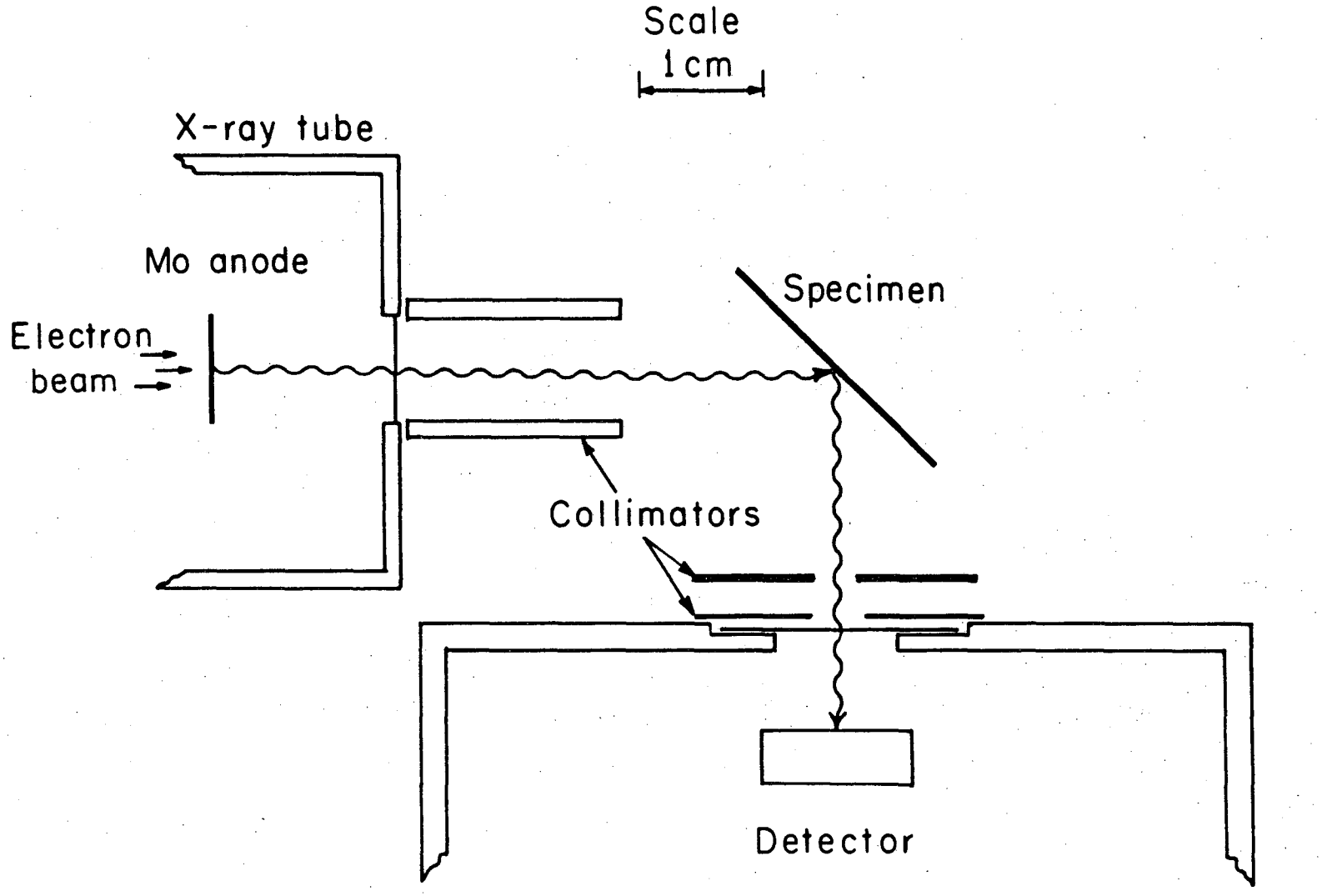
Scale
1 cm
X-ray tube
Mo anode
Electron
beam
Specimen
Collimators
Detector
XBL747-3765

Fig. 3

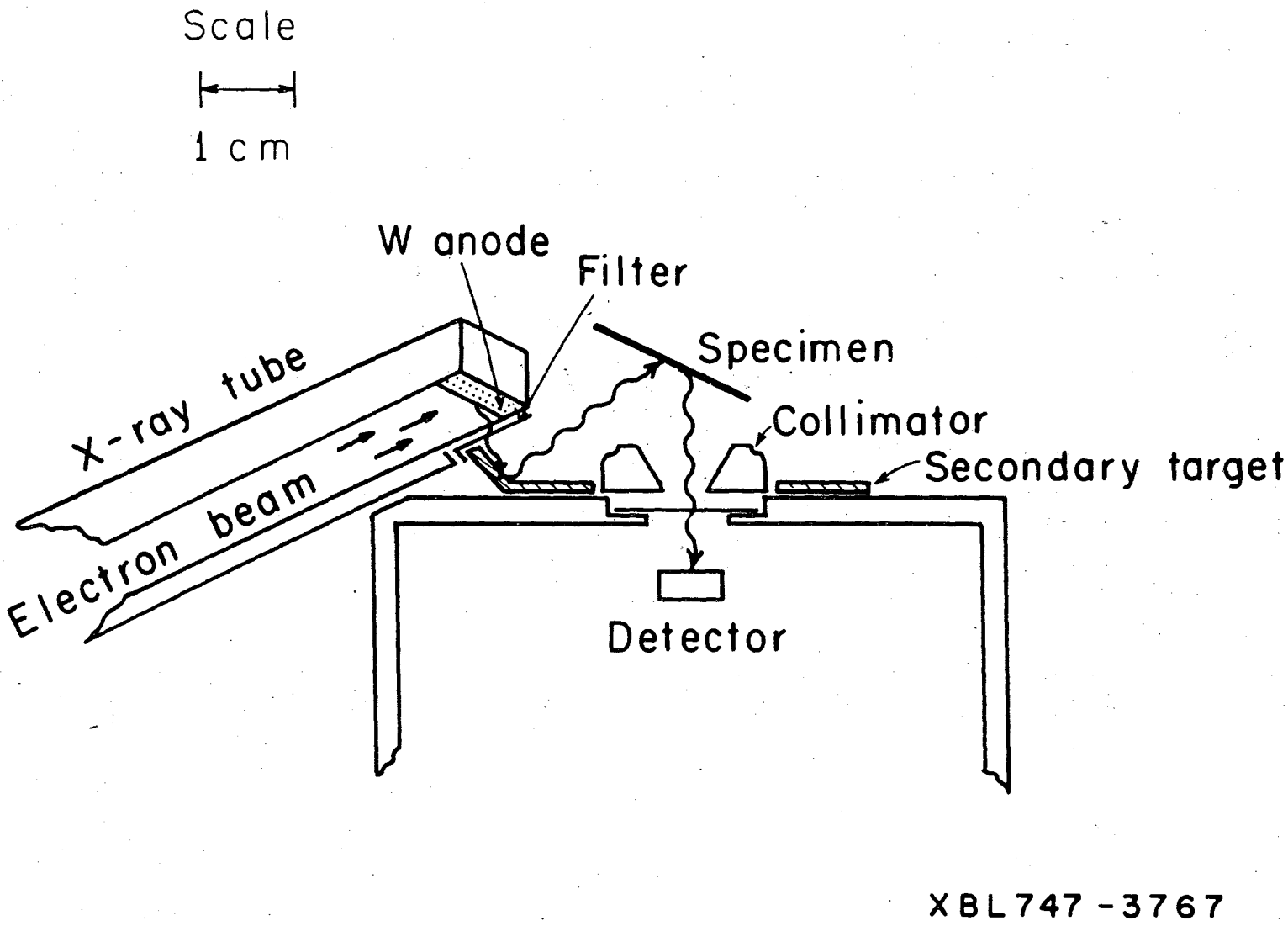

Fig. 4

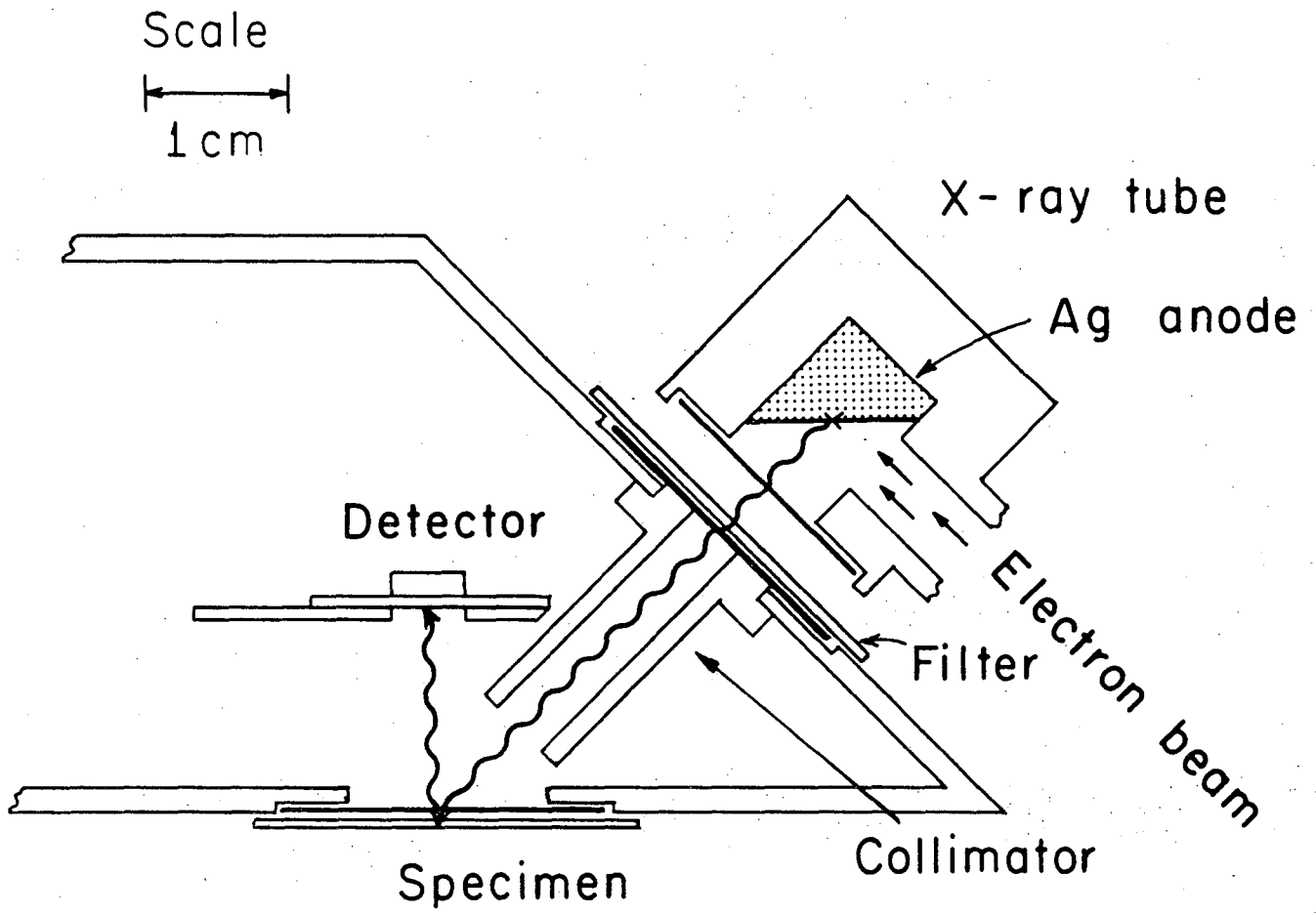
Scale
1 cm
X-ray tube
Ag anode
Detector
Electron beam
Filter
Collimator
Specimen
XBL747-3768

Fig. 5

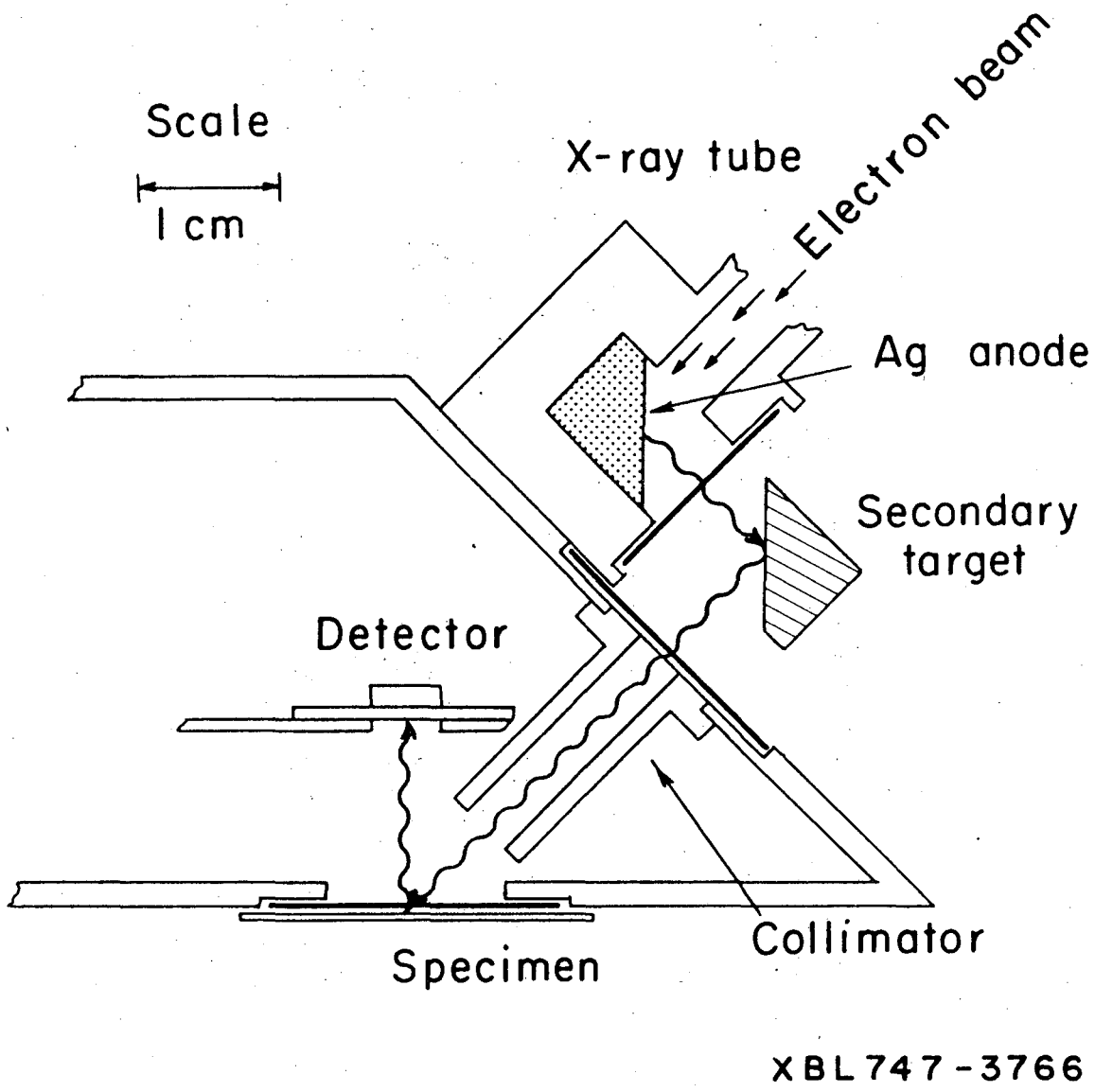
Scale
1 cm
X-ray tube
Electron beam
Ag anode
Secondary target
Detector
Collimator
Specimen
XBL747-3766

Fig. 6

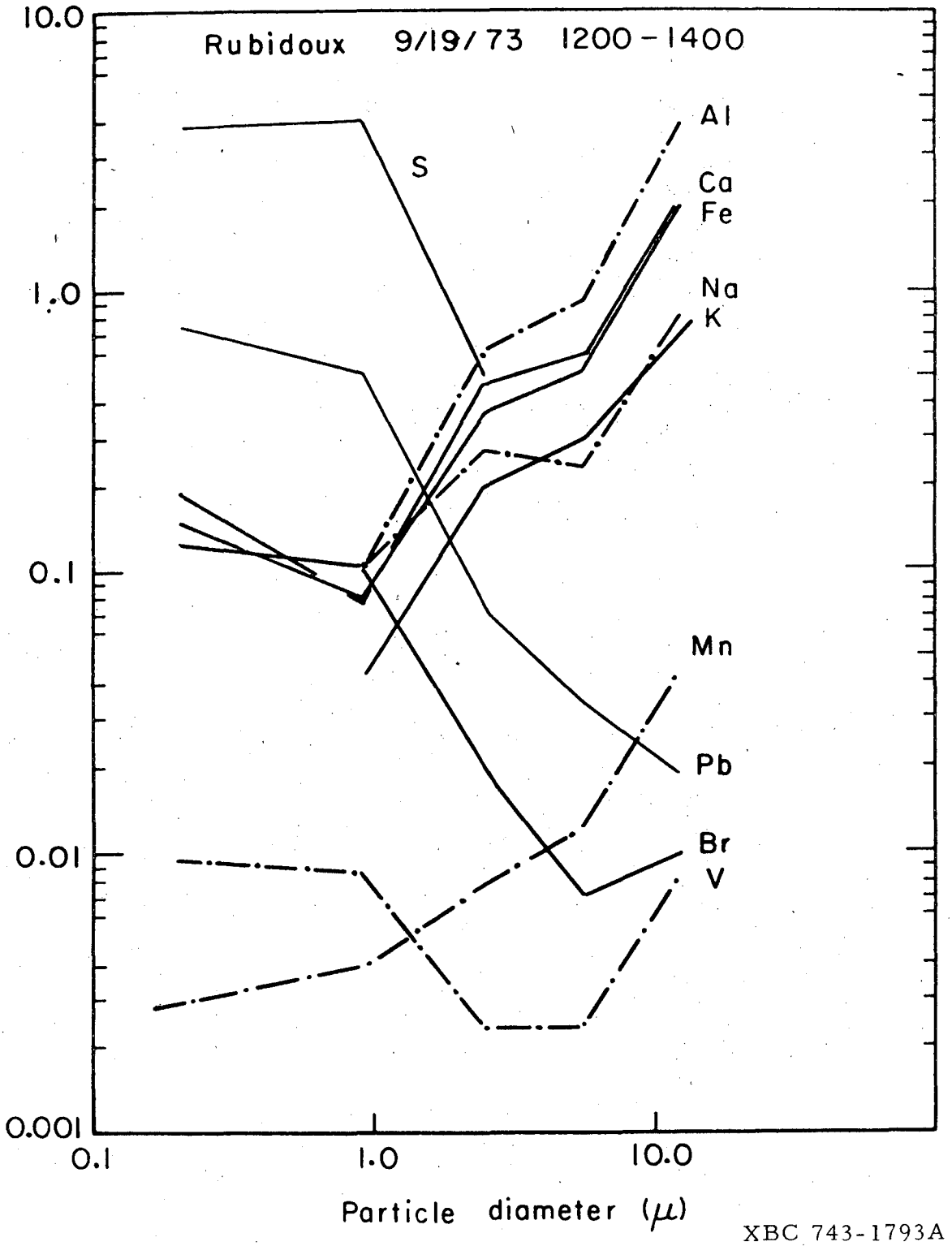
Rubidoux 9/19/73 1200-1400
10.0
1.0
0.1
0.01
0.001
0.1
1.0
10.0
Particle diameter (μ)
S
Al
Ca
Fe
Na
K
Mn
Pb
Br
V
XBC 743-1793A

Fig. 7

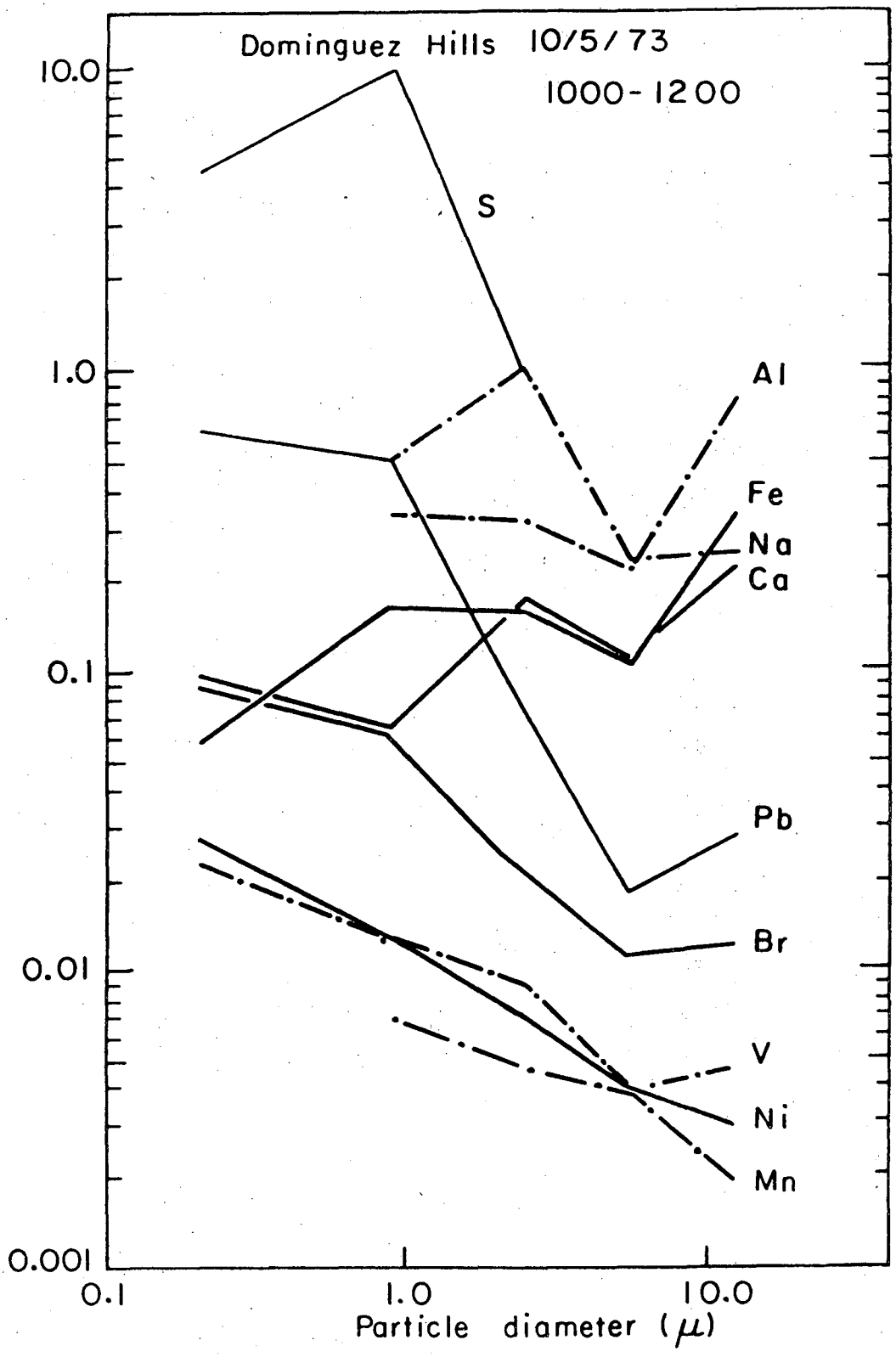

XBC 743-1796A

Fig. 8

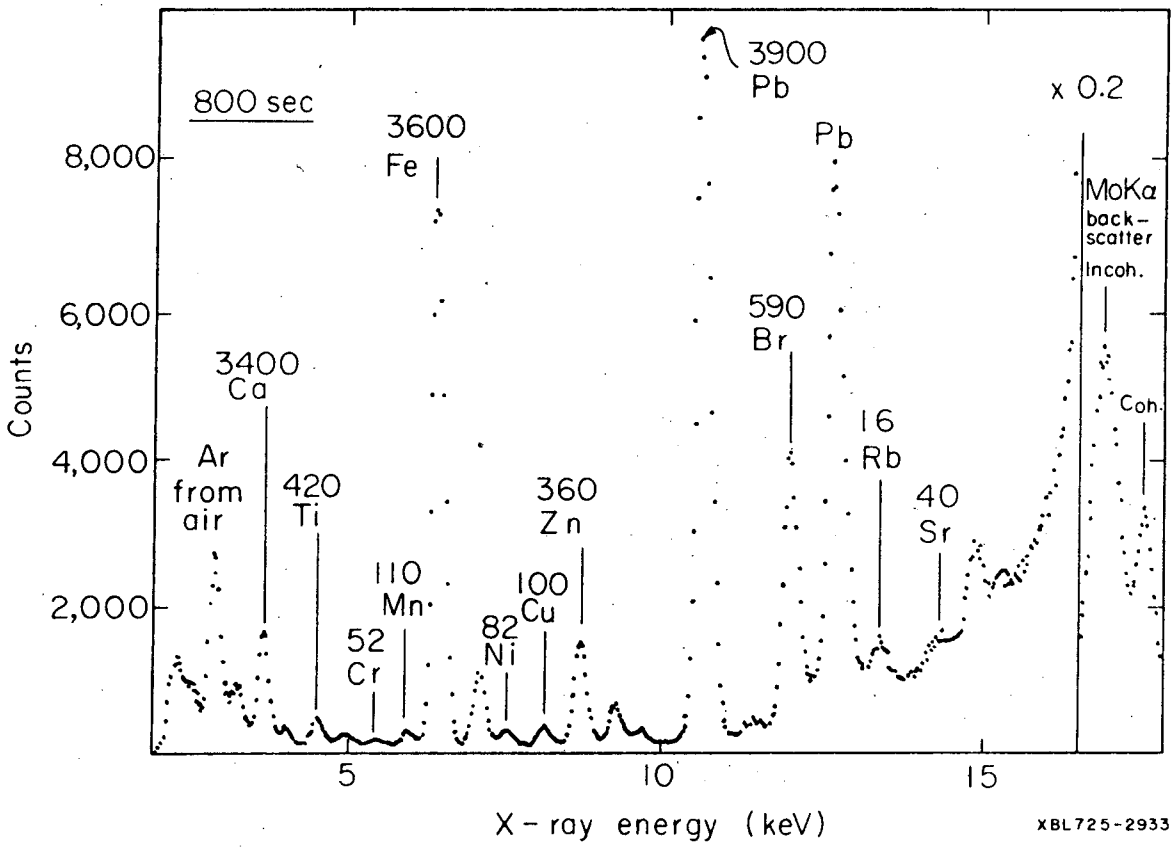
800 sec
3600
Fe
3900
Pb
x 0.2
Pb
MoKα
back-
scatter
Incoh.
Coh.
590
Br
16
Rb
40
Sr
3400
Ca
Ar
from
air
420
Ti
360
Zn
110
Mn
52
Cr
82
Ni
100
Cu
8,000
6,000
4,000
2,000
Counts
5
10
15
X-ray energy (keV)
XBL725-2933

Fig. 9

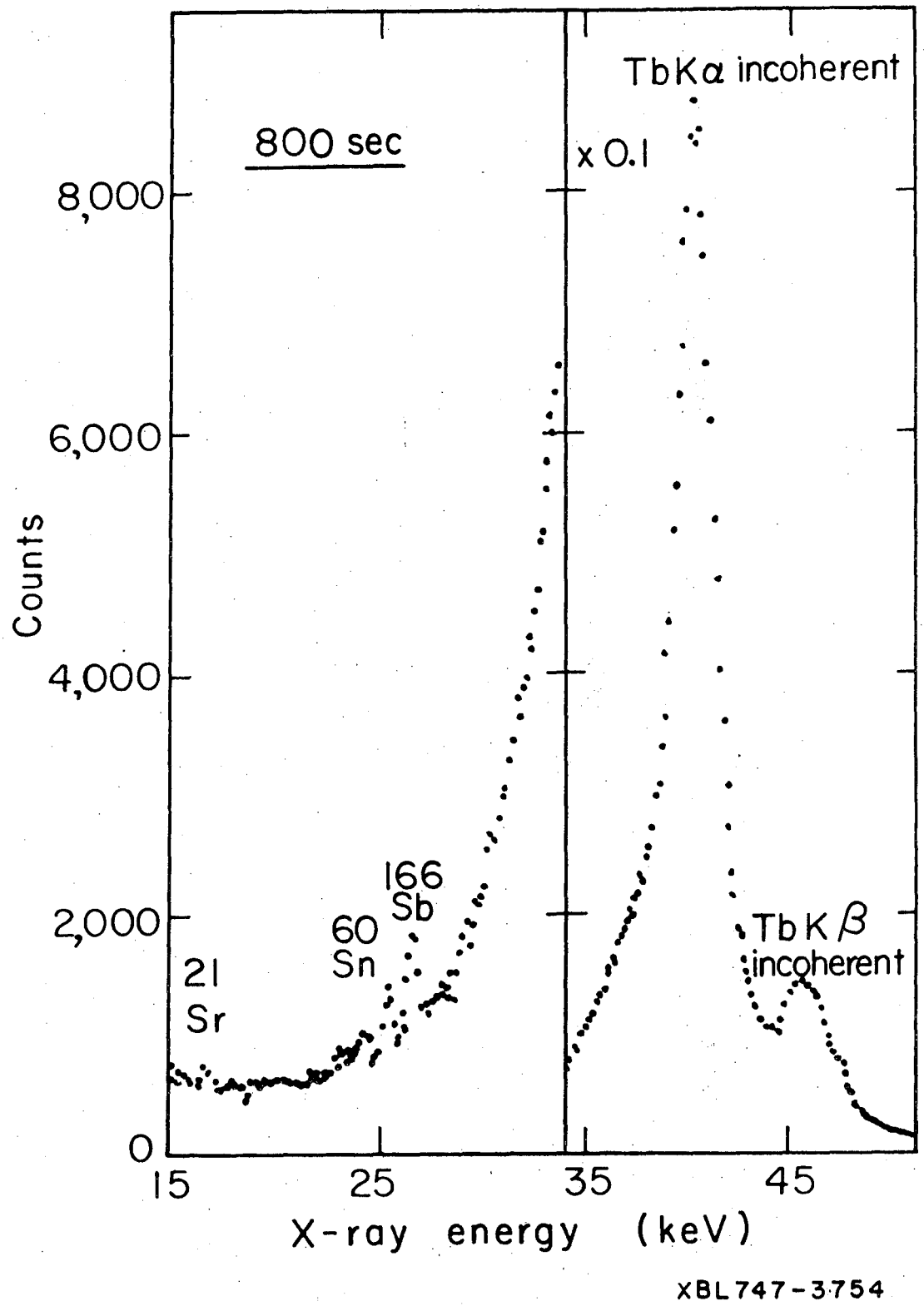

Fig. 10

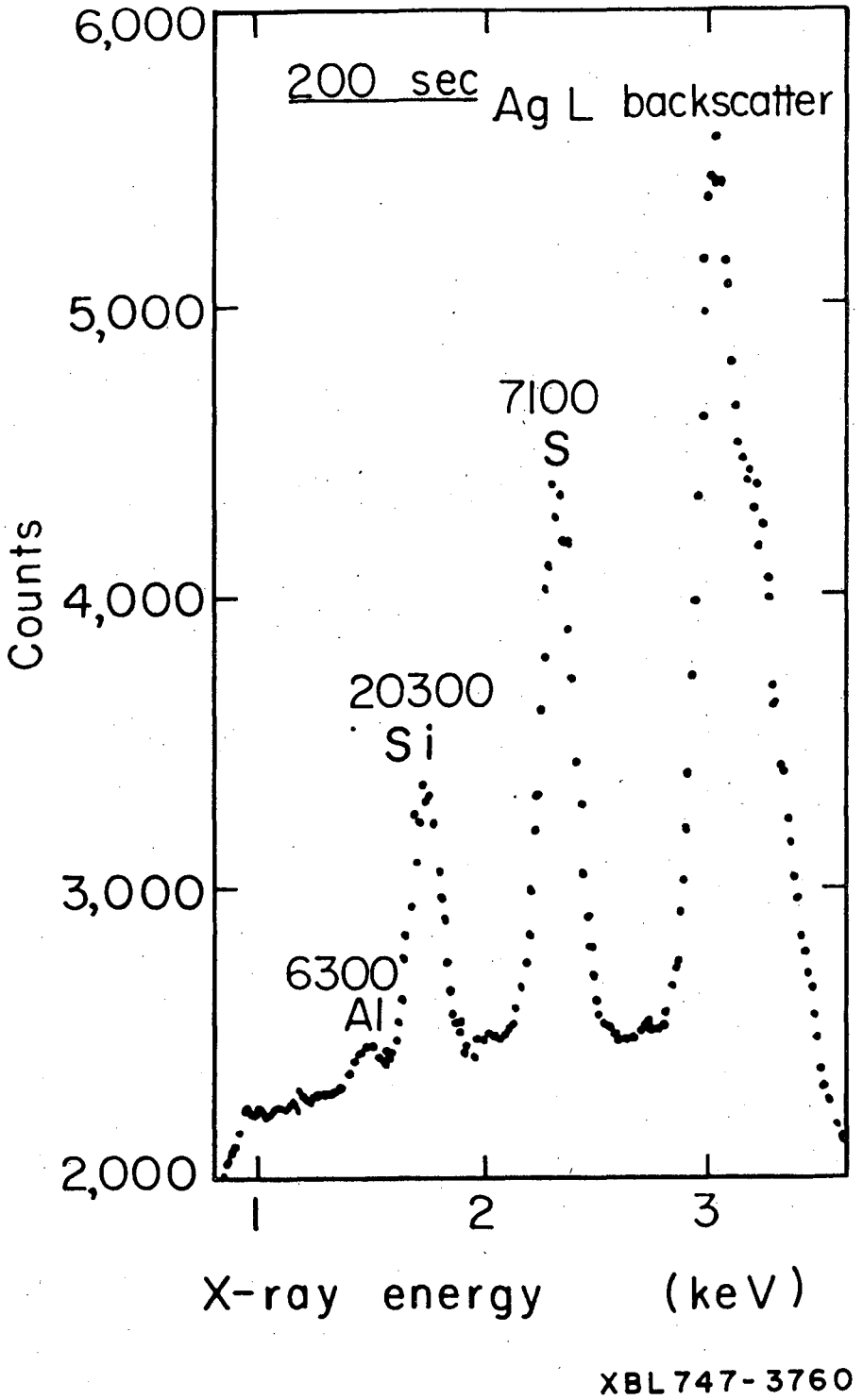
6,000
5,000
4,000
3,000
2,000
Counts
200 sec
Ag L backscatter
7100
S
20300
Si
6300
Al
1
2
3
X-ray energy (keV)
XBL747-3760

Fig. 11

TECHNICAL INFORMATION DIVISION
LAWRENCE BERKELEY LABORATORY
UNIVERSITY OF CALIFORNIA
BERKELEY, CALIFORNIA 94720